High-quality graphene on SiC(000$\bar{1}$) formed through an epitaxial TiC layer

Keisuke Kimura,[1] Kentaro Shoji,[1] Yuta Yamamoto,[3] Wataru Norimatsu,[1,2] and Michiko Kusunoki[2,3,*]

[1]*Department of Applied Chemistry, Nagoya University, Nagoya-shi, Aichi-ken, 464-8603, Japan*

[2]*Materials Research and Development Laboratory, Japan Fine Ceramics Center, Nagoya-shi, Aichi-ken, 456-8587, Japan*

[3]*EcoTopia Science Institute, Nagoya University, Nagoya-shi, Aichi-ken, 464-8603, Japan*

(Received 3 July 2012; revised manuscript received 11 December 2012; published 20 February 2013)

The formation of large-area homogeneous graphene on a C-terminated SiC (000$\bar{1}$) surface was achieved via decomposition of the SiC (000$\bar{1}$) surface covered with an ultrathin but much more stable TiC layer than the reactive SiC(000$\bar{1}$). By heating the SiC (000$\bar{1}$) surface with a mixed powder of TiO_2 and carbon at 1500–1550 °C in vacuum, an extremely homogeneous, epitaxial 0.75-nm-thick TiC(111) layer was grown on the SiC(000$\bar{1}$) surface over a millimeter-scale area. Graphitization of the TiC-masked SiC surface led to the growth of high-quality graphene layers, which consist of TiC- and SiC-derived carbon. High-resolution transmission electron microscopy revealed the presence of disordered stacking of graphene layers on SiC through an amorphous layer at the interface. This unique method will promise further progress of relatively high carrier mobility of graphene formed on the SiC (000$\bar{1}$) surface.

DOI: 10.1103/PhysRevB.87.075431 PACS number(s): 61.48.Gh, 68.37.Og, 81.05.ue

I. INTRODUCTION

Graphene, the one-atom-thick carbon material having a hexagonal honeycomb lattice, has attracted much attention owing to its excellent intrinsic properties.[1,2] The electronic properties of graphene are characterized by massless Dirac fermions and a room temperature quantum Hall effect, resulting in an extremely high carrier mobility at room temperature.[3,4] For high-frequency electronic applications that exceed the performance of Si-MOSFET technology, it will be necessary to produce graphene that is homogeneous and of high-quality crystallinity over a large area.

The thermal decomposition of SiC is expected to form graphene layers homogeneously at a wafer scale. In this method, annealing in a vacuum or in an Ar atmosphere leads to the preferential sublimation of Si atoms from the SiC{0001} surface, resulting in epitaxial graphene growth of the remaining C atoms.[5–7] This enables the self-organization of graphene on a semi-insulating substrate. Previous transmission electron microscopy (TEM) observations have revealed the peculiar interface structures and the selective stacking sequence of graphene on SiC(0001), which are responsible for its distinct electronic properties.[8–10] Hexagonal SiC crystals have a polar *c* axis, which generates two opposite {0001} surfaces: the Si-terminated (0001) face and the C-terminated SiC(000$\bar{1}$) face. It has been reported that graphene layers formed on these two faces have different structures and that their electronic properties differ due to difference in reactivity.[11] In graphene formed on the Si-face, a fraction of the C atoms in the first carbon layer adjacent to the SiC substrate makes covalent bonds with the Si atoms at the interface, leading to the formation of a buffer layer of a $(6\sqrt{3} \times 6\sqrt{3})R30^\circ$ surface reconstruction.[7,8] This strong interaction with the substrate is considered to decrease the mobility of graphene on the Si face.[7,9,12,13] However, concerning the morphology, the buffer layer $(6\sqrt{3} \times 6\sqrt{3})R30^\circ$ appears to act as a template layer for graphene growth on the SiC(0001) face, ensuring well-ordered graphene on the substrate. Recently, it was reported that the buffer layer on the Si face can be successfully cleaved from the substrate via hydrogen intercalation.[14,15] Although this is expected to be an attractive process for the improvement of the electronic properties of graphene on the Si-face, it is not easy to remove all of the buffer layer in order to increase the mobility drastically.[16]

On the other hand, the SiC(000$\bar{1}$) face is known to have a higher chemical activity than the SiC(0001) face. We previously reported that well-aligned carbon nanotubes are formed on the SiC(000$\bar{1}$) face in an active oxidation atomosphere.[5] Even in ultrahigh vacuum or Ar atmosphere, thicker graphene forms on the (000$\bar{1}$) face than (0001) face for a given annealing time and temperature.[17,18] It is now widely understood that on the (000$\bar{1}$) face, no template layer such as the $(6\sqrt{3} \times 6\sqrt{3})R30^\circ$ surface structure on (0001) face forms, and then the interaction with the substrate is weak, leading to the presence of rotational disorder on the (000$\bar{1}$) face. The rotational disorder leads to a linear (Dirac type) band dispersion close to the *K* point and to a high mobility for graphene formed on the (000$\bar{1}$) face.[13,19–21] The electronic properties of the multilayer graphene films produced on the (000$\bar{1}$) face resemble those of single monolayer graphene, even for films consisting of many monolayers.[19] However, the grain size is small and defective, and the number of graphene layers easily changes on the SiC(000$\bar{1}$) face.

We have previously reported a feature of the formation mechanism of graphene on the SiC(000$\bar{1}$) C-face in which, in the initial stage of the decomposition, the surface is roughened, and multilayered arced nanometer-sized regions of graphene are formed in craters that act as nuclei for graphene growth on the terraces of the SiC(000$\bar{1}$). However, this phenomenon essentially induces inhomogeneity of decomposition, resulting in roughness and a random arrangement of the number of graphene layers on the SiC(000$\bar{1}$) face.

To suppress this phenomenon on the reactive SiC(000$\bar{1}$) C-face, it is important that more suppressed decomposition starts at as high a temperature as possible on a flat terrace because the higher the decomposition temperature, the larger the lateral growth rate of graphene. Previously, for this purpose, an Ar ambient,[22] a high-pressure Ar atmosphere,[23] or sublimation in a confined space[24] have been applied, but these measures

cannot be said to have been sufficient for the decomposition of the SiC(000$\bar{1}$) C-face.

In the work described here, we tried to restrain the generation of irregular nucleation and craters of graphene on the SiC(000$\bar{1}$) C-face at a low temperature by depositing in advance an ultrathin epitaxial film of the stabler carbide, TiC, as an effective stabilizing layer for the reactive SiC(000$\bar{1}$) C-face. By this method, we have succeeded in forming homogeneous graphene on the on-axis SiC(000$\bar{1}$) C-face.

II. EXPERIMENTAL PROCEDURE

On-axis 6H-SiC(000$\bar{1}$) single-crystal wafers that had been subjected to chemical and mechanical polishing were cut into 1×2 mm^2 pieces and cleaned ultrasonically in acetone and ethanol. These substrates were heated to 1500–1550 °C for 0.5 h in a vacuum of 1×10^{-4} Torr with a 10:4 powder mixture of TiO_2-to-carbon in a carbon crucible. The crucible was placed in a furnace with an electrical resistance carbon heater with a SiC powder also set around the crucible to restrain the decomposition of SiC under the TiC layer. The coexisting SiC powder (average diameter of 2 μm) in the crucible was effective in preventing the decomposition of SiC. The SiC powder has a higher active surface and specific surface area than SiC single crystal substrates and therefore starts to decompose earlier than the SiC substrate, thereby supplying Si vapor to the atmosphere around the SiC substrate.

The TiC/SiC(000$\bar{1}$) substrates were further annealed at 1500 °C for 0.5 h or 1.5 h in an Ar atmosphere of 6 atm pressure for surface graphitization. This arrangement was effective in suppressing decomposition due to the oxidation reaction of the carbides with a small amount of residual oxygen in the furnace. The purity of the Ar gas used was more than 99.9999%. Details were described in our previous paper.[23] Specimens for TEM along the cross-sectional direction were prepared by a conventional Ar ion-thinning method. Atomic force microscope (AFM) measurements were carried out using a Shimadzu SPM-9700 scanning probe microscope. TEM observations were carried out using a Topcon EM-002B and a JEM-ARM200F at accelerating voltages of 200 kV and 120 kV. Micro-Raman spectroscopic analysis was performed on a Renishaw inVia Reflex Raman microscope with a 532-nm laser excitation source.

III. RESULTS AND DISCUSSIONS

A. Formation of a thin TiC film on a SiC substrate

Figure 1 shows a TEM image of a TiC particle annealed at 1700 °C for 0.5 h in a vacuum. We can confirm the formation of several layers of well-crystallized epitaxial graphene on preferentially grown TiC(111) or (100) surfaces by the thermal decomposition of TiC, similar to that of SiC. This result also shows that TiC is much more stable than SiC because over 20 layers of graphene are formed by annealing SiC under the same condition, even in an Ar atmosphere.[23] TiC should start to decompose at a higher temperature than SiC. Following this result, we decided to use a TiC crystal as a stabilizing layer of the SiC surface to restrict SiC(000$\bar{1}$) surface decomposition. Furthermore, the crystal structure of TiC is of the NaCl type ($a = 4.3218$ Å), and the sites of Ti atoms (or C atoms) with

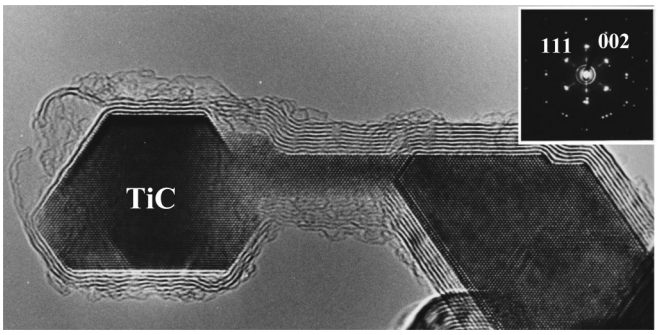

FIG. 1. TEM image of graphene layers formed on the facets grown around a TiC particle annealed at 1700 °C in a vacuum.

threefold symmetry projected on TiC(111) and Si atoms (or C atoms) projected onto the 6H-SiC(000$\bar{1}$) surface are almost coincident, as shown in Fig. 2. The lattice mismatch between the 6H-SiC(0001) and TiC(111) is 0.97%, which is favorable for forming a coherent and homogeneous interface between the two layers. The surface energy ratio estimated with a simple hard sphere model of the (111), (100), and (110) planes of TiC is 0.186:0.214:0.303 due to coordination effects. Thus, it is also expected that the lowest surface energy TiC(111) surface will grow preferentially, leading to the epitaxial formation of a homogeneous TiC layer over a large area of the SiC substrate.

We first investigated the optimum conditions needed to form a TiC thin film on the SiC(000$\bar{1}$) C-face by heating the SiC substrate with a mixed powder of TiO_2 and carbon. TiO_2 starts to decompose below 1000 °C in vacuum, and oxygen gas is supplied with Ti vapor in the crucible. Then, we assume that the carbon powder is oxidized and CO gas is produced. The thin TiC layer is then formed on the SiC surface at the relatively low temperature through the reaction as follows:

$$TiO_2 + 2C \rightarrow Ti + 2CO$$
$$2Ti + 2CO \rightarrow 2TiC + O_2$$

Figure 3(a) shows a scanning electron microscopy (SEM) image of the surface heated at 1600–1650 °C for 1 h in the carbon crucible in vacuum. Oriented blocks about 400–500 nm in size are connected parallel to the SiC substrate. Figures 3(b) and 3(c) are a TEM image and an electron diffraction pattern of the blocks on the SiC(000$\bar{1}$) C-face observed along the

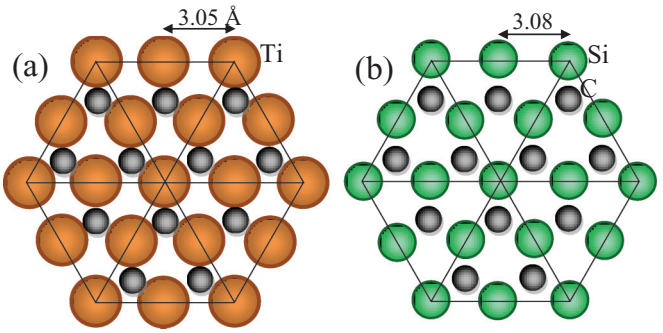

FIG. 2. (Color online) Projected sites of (a) Si atoms (or C atoms) on 6H-SiC(000$\bar{1}$) and (b) Ti atoms (or C atoms) on TiC(111).

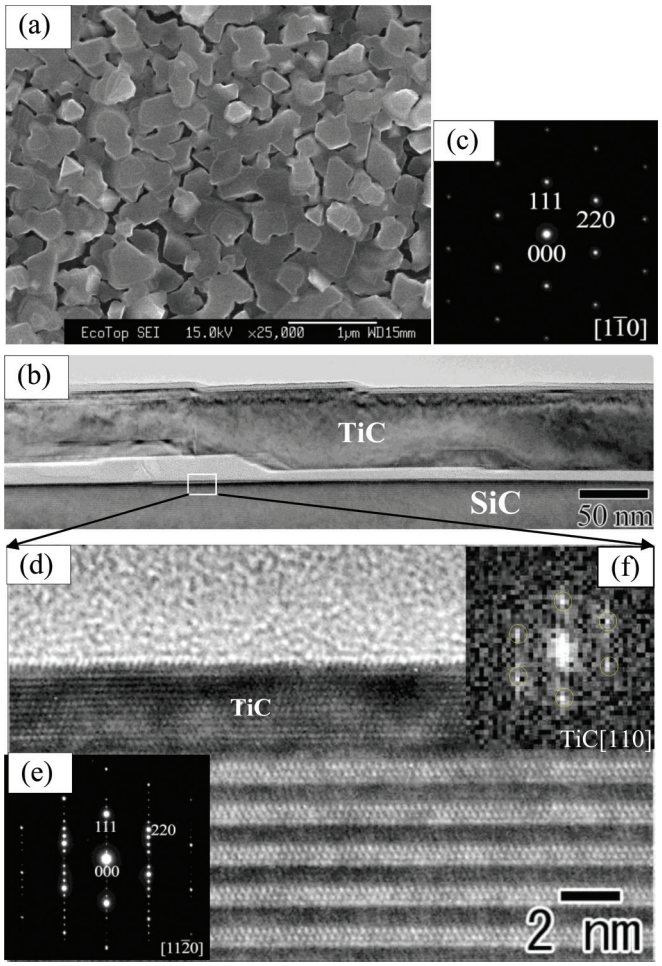

FIG. 3. (Color online) TiC blocks and layer formed on the SiC(000$\bar{1}$) at 1600–1650 °C for 1 h. (a) SEM image of the TiC connected blocks. (b), (c) TEM images of the TiC blocks and the electron diffraction pattern. (d) The high-resolution TEM image, (e) the electron diffraction pattern, and (f) the FFT pattern of the TiC layer formed on the SiC(000$\bar{1}$) face.

cross-sectional direction. These results revealed that the blocks were TiC crystals 50–100 nm thick. Simultaneously, black-contrast layers about 3-nm thick are formed homogeneously on the surface of the SiC substrate under the large blocks in the high resolution TEM image shown in Fig. 3(d). The electron diffraction pattern and the fast Fourier transform (FFT) pattern of the lattice image, shown in Figs. 3(e) and 3(f), respectively, revealed that the black-contrast layer is also composed of TiC. The orientation relationship between the TiC layers (also TiC blocks) and SiC was SiC(000$\bar{1}$)//TiC(111), TiC[1$\bar{1}$0]//SiC[11$\bar{2}$0].

To form a much larger area and homogeneous ultrathin TiC layer on the SiC(000$\bar{1}$) C-face without formation of the TiC blocks, the reaction temperature was decreased by 100 °C. Figure 4 shows (a) a low-magnification and (b) an enlarged high-resolution TEM image of the reacted SiC(000$\bar{1}$) C-face at 1500–1550 °C for 1 h in a vacuum. A dark contrast corresponding to a 0.75-nm-thick TiC layer is observed on the surface of the SiC substrate, as shown in Fig. 4(b). This ultrathin TiC layer had a homogeneous thickness and the interface between TiC and SiC was extremely flat over the whole terrace, as shown in Fig. 4(a).

Figures 4(c) and 4(d) show AFM images of the SiC(000$\bar{1}$) C-face before and after heat treatment with a mixed powder of TiO_2 and carbon at 1500–1550 °C for 1 h in a vacuum, respectively. We can see that the pristine SiC(000$\bar{1}$) C-face scratched by mechanical polishing shown in Fig. 4(c) became drastically smooth after the growth of the TiC layer, as shown in Fig. 4(d). Observing the TiC /SiC(000$\bar{1}$) surface in a millimeter scale by an optical microscope, rough surface areas were often observed as a bright contrast, as shown by arrows in Fig. 4(e). However, by controlling the total amounts of the mixed powder of TiO_2 and C in the carbon crucible, we finally succeeded in enlarging the homogeneously flat TiC/SiC(000$\bar{1}$) surface area to an area of 1×2 mm^2, as shown in Fig. 4(f). This result indicates that over 1500 °C, the deposited surface atoms of TiC can move easily and preferentially grow a thin layer of TiC(111) having the lowest surface energy. Simultaneously, SiC actively diffuses under the thin, flat but hard and stable TiC layer without decomposition even at such a high temperature, leading to the formation of a smooth TiC/SiC interface.

Figure 5(a) shows the TEM bright field image of the TiC layer on the SiC(000$\bar{1}$) C-face and the corresponding electron energy loss spectroscopy (EELS) mapping images of the (b) C and (c) Ti elements. This result shows that Ti atoms exist only in a thin surface area with a depth corresponding to the width of the dark contrast area in the bright field image shown in Fig. 5(a).

B. Graphitization of the thin TiC film on the C-terminated SiC substrate

Subsequently, the TiC-layered SiC(000$\bar{1}$) C-face was graphitized by thermal decomposition. Figures 6(a) and 6(b) show TEM images of the graphene layers formed by annealing the TiC-layered SiC(000$\bar{1}$) C-face at 1500 °C for 0.5 and 1.5 h in Ar gas at 6 atm pressure, respectively. In Fig. 6(a), five layers of graphene were formed in the main; however, remaining TiC layers were sometimes observed as shown by an arrow on the left side of the image. In Fig. 6(b), six layers of graphene were formed all over the surface with no TiC layers remaining. Figures 6(c) and 6(d) are an AFM topographic image and the corresponding phase image of the same sample shown in Fig. 6(b), respectively. The topographic image with a cross-sectional cut along the line A-B in (c) shows that the periodical morphology of steps 1.0–1.5 nm in height is maintained after graphitization and the contrast of each terrace is homogeneous, though the edge of the steps is not straight. The contrast of the phase image shown in Fig. 6(d) is also rather homogeneous, at least in the area of 1–2 μm. It has been reported that AFM phase images reflect sensitively layered numbers of graphene.[25] Therefore, these results of the TEM and AFM images confirm that multilayer graphene is homogeneously formed over areas of hundreds of nm to a few micrometers. Previous works[11,26] using AFM and low energy electron microscope have reported that graphene formed on the SiC(000$\bar{1}$) C-face in vacuum contains often small grains under 100 nm in size, and the one formed in argon shows inhomogeneous coverage (0–6 layers) on the random substrate

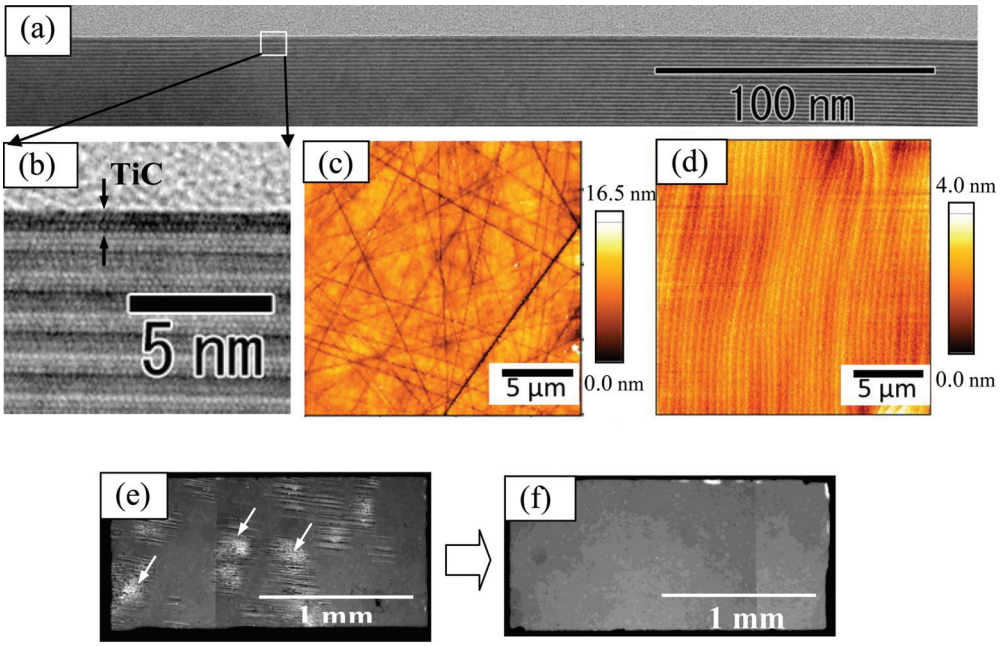

FIG. 4. (Color online) Ultrathin TiC layer formed on the SiC(000$\bar{1}$) C-face at 1500–1550 °C for 1 h. (a) Low-magnification TEM image and (b) high-resolution TEM image of the ultrathin TiC layer on SiC observed along the cross-sectional direction. AFM images of (c) the mechanically polished surface of the as-received SiC(000$\bar{1}$) C-face and (d) the ultrathin TiC-layered SiC surface. Optical microscopy images of (e) uncontrolled and (f) well-controlled TiC-layered SiC surfaces of millimeter size.

morphology before complete graphene coverage is achieved. Accordingly, it can be said that the present method using the TiC epitaxial layer is rather effective to grow multilayer graphene maintaining the initial step-terrace topography.

To show the quality of graphene, a Raman spectrum of the graphene layers is shown in Fig. 6(e). The spectrum was corrected for the emission of the substrate by subtraction. *G* and *2D* peaks were observed at 1589 and 2710 cm^{-1}, respectively. Full-width at half-maximum of the *2D* peak was 52 cm^{-1}. A *D* peak at 1356 cm^{-1} was very weak. Comparing it with the previous report about the dependence of Raman spectra intensity and broadness on layer numbers of single- and multilayered graphene,[27,28] the obtained result presents well the formation of high-quality multilayered graphene on SiC(000$\bar{1}$).

The graphene layers ought to be derived from TiC and SiC. Here, in the TiC(111) planes, two-dimensional C-atom and Ti-atom layers, as shown in Fig. 1(b), are stacked alternately with a spacing of $d_{111}/2$ ($d_{111} = 0.248$ nm) along the [111] direction. The C atom density in one C-atom layer of TiC(111) is about one third of that of graphene, which is almost the same as that of one SiC bilayer in the SiC(0001). That is, one layer of graphene is formed by decomposing three C atom layers of the TiC(111). The thickness of the TiC layer was 0.75 nm, as shown in Fig. 4(b). That is, the TiC layer contains about three C atom layers. This means that only the first upper layer of graphene is derived from TiC and the lower several layers are from the SiC substrate.

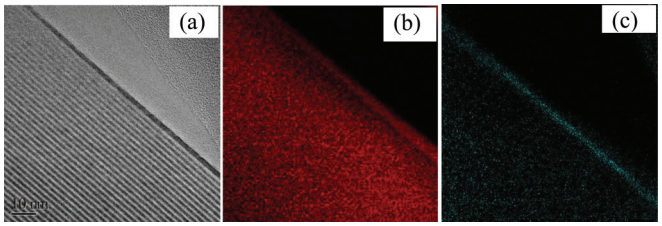

FIG. 5. (Color online) EELS mapping images of the TiC/SiC substrate. (a) The bright field TEM image; (b) C mapping; (c) Ti mapping.

A high-resolution TEM observation was carried out along the [1$\bar{1}$00] direction of SiC parallel to the [11$\bar{2}$0] of graphene. Along this direction, we can distinguish image contrasts of the graphite structures with AAA, ABA, and ABC stacking sequences due to the difference in the extinction rules between them in electron diffraction patterns. In this way, we previously reported that graphene formed on the SiC(0001) Si-face selectively adopts the ABC stacking sequence structure.[10] In the high-resolution TEM image shown in Fig. 7(a), alternate dark lines and white dotted lines are clearly observed, which reflect the stacking sequence of graphene layers. The occurrence of a particular stacking sequence does not seem necessarily to be consistent. Figure 7(b) shows the FFT pattern of the graphene lattice image shown in Fig. 7(a). The reflections in the rows shown by red arrows, which correspond to that from graphene layers in the image, are strongly streaked and have multiple maxima of intensity, as shown by small arrows. This result shows that graphene formed by the decomposition of the TiC layered SiC(000$\bar{1}$) C-face has a slightly disordered stacked structure shifted along the (000$\bar{1}$) plane of graphene. It cannot be discerned from the cross-sectional TEM image whether the disordered stacked structure is caused by the rotational disordering generally seen on the SiC(000$\bar{1}$) C-face, because of the insensitivity of TEM images to a slight tilting angle of samples to the electron beam. However, the slightly

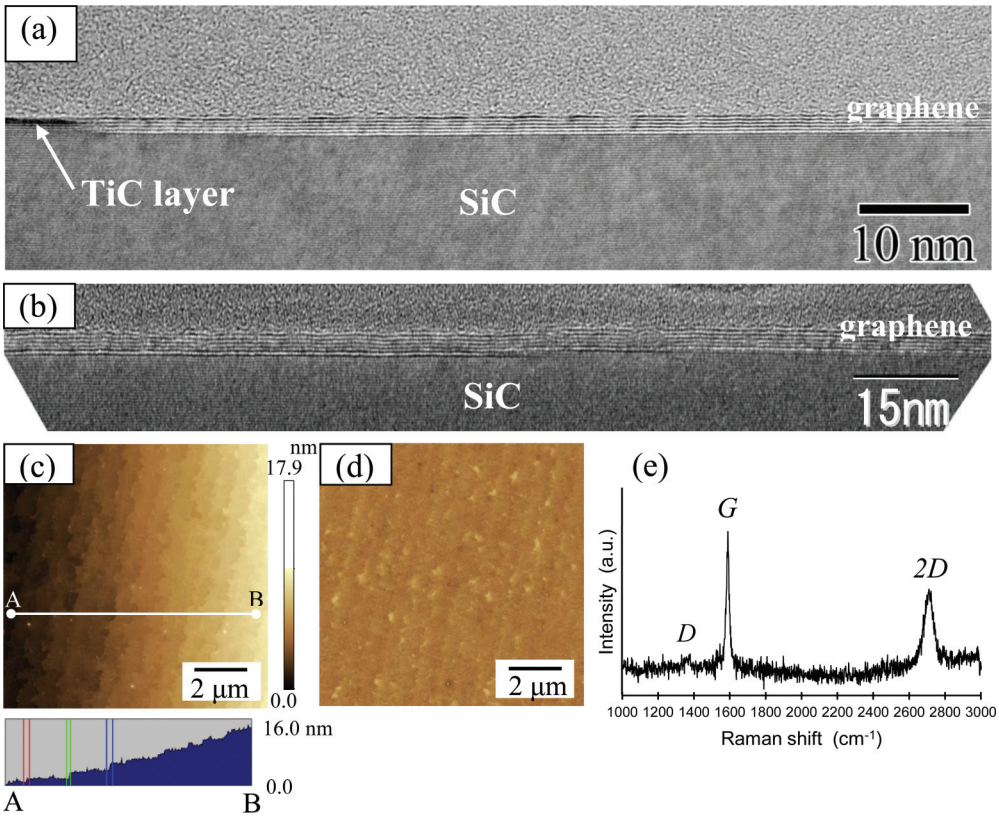

FIG. 6. (Color online) TEM images of homogeneous high quality graphene layers formed by graphitization of the TiC/SiC(000$\bar{1}$) C-face at 1500 °C (a) for 0.5 and (b) for 1.5 h in Ar gas at 6 atm pressure. (c) AFM topographic image with the cross-sectional cut along the line A-B, and (d) the corresponding phase image of the same sample shown in (b). (c) Heights of the steps sandwiched by red, green, and blue parallel lines were 0.93, 1.55, and 1.51 nm, respectively. (e) Raman spectrum at 532 nm for the graphene layers shown in (b), (c), and (d).

disordered stacked structure at least indicates that the degree of the interaction between each graphene layer obtained from the TiC/SiC C-face is weak. Lattice contrast of graphene layers in cross-sectional TEM images on the SiC(000$\bar{1}$) C-face is generally slightly fluctuate,[23] which is presumed to be due to the presence of stacking disordering. On the other hand, the contrast of graphene formed on the TiC/SiC C-face shown in Figs. 6(a), 6(b) and Fig. 7(a) is relatively homogeneous and distinct. The top graphene layer derived from the TiC layer that is formed first is thought to be flat, which is similar to the homogeneous graphene formed on the SiC(0001) Si-face, which is formed layer-by-layer at a higher temperature than that on the SiC(000$\bar{1}$) C-face. Hence, the first layer of graphene derived from the TiC layer would effectively suppress the formation of the craters by decomposition of the active SiC(000$\bar{1}$) C-face, and then defects or disordering in the graphene layers would decrease compared with those generally formed on SiC(000$\bar{1}$) C-face. However, the graphene layers bonded loosely with the SiC substrate and were more easily peeled from the substrate during TEM sample preparation than the graphene layers formed on SiC(0001) Si-face. In Fig. 7(a), we can just observe an amorphous layer at the interface between the graphene and the SiC surface shown by a yellow arrow, which is known to be a feature of graphene formed on the C-face.

Further, in order to apply graphene to extremely high speed electronic and optoelectronic devices, the specific contact resistances at the metal/graphene interface, which

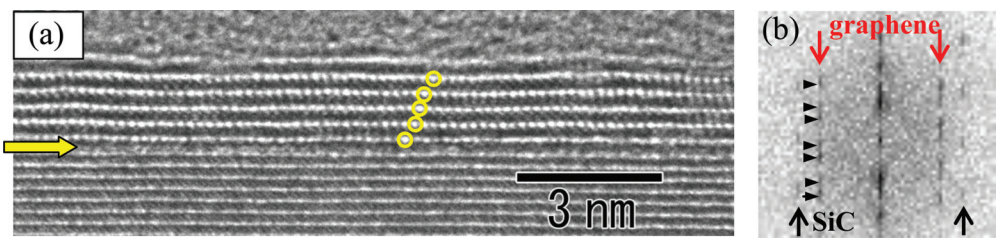

FIG. 7. (Color online) (a) High-resolution TEM image of the graphene formed from the ultrathin TiC layer/SiC(000$\bar{1}$) C-face observed along graphene [11$\bar{2}$0] direction//SiC[1$\bar{1}$00]. (b) FFT pattern of the disordered stack-structured graphene layers on SiC.

are currently reported to be on the order of 5×10^{-6} Ω cm^2,[29,30] need to be considerably decreased. Though it was recently reported to have been improved to 10^{-7} Ω cm^2, graphene had to be exposed to plasma treatment to achieve this value.[31] To this end, the undecomposed area of the TiC layer, shown by the arrow in Fig. 6(a), offers a possibility of playing a role in forming high quality ohmic contacts to graphene by leaving TiC areas partially as electrodes.

IV. CONCLUSIONS

An homogeneous ultrathin epitaxial TiC layer of millimeter size could be formed on the SiC(000$\bar{1}$) C-face by annealing the C-face with TiO_2 and carbon powders in vacuum. Graphitizing the C-face masked by this TiC layer produced extremely homogeneous and high quality graphene layers over a large area. This unique process has the promise to allow the production of graphene with high carrier mobility on the SiC(000$\bar{1}$) C-face.

*Corresponding author: kusunoki@esi.nagoya-u.ac.jp

[1] K. S. Novoselov, A. K. Geim, S. V. Morozov, D. Jiang, Y. Zhang, S. V. Dubonos, I. V. Grigorieva, and A. A. Firsov, Science **306**, 666 (2004).
[2] A. K. Geim and K. S. Novoselov, Nat. Mater. **6**, 183 (2007).
[3] K. S. Novoselov, A. K. Geim, S. V. Morozov, D. Jiang, M. I. Katsnelson, I. V. Grigorieva, S. V. Dubonos, and A. A. Firsov, Nature (London) **438**, 197 (2005).
[4] S. V. Morozov, K. S. Novoselov, M. I. Katsnelson, F. Schedin, D. Elias, J. A. Jaszczak, and A. K. Geim, Phys. Rev. Lett. **100**, 016602 (2008).
[5] M. Kusunoki, T. Suzuki, T. Hirayama, N. Shibata, and K. Kaneko, Appl. Phys. Lett. **77**, 531 (2000).
[6] C. Berger, Z. Song, X. Li, X. Wu, N. Brown, C. Naud, D. Mayou, T. Li, J. Hass, A. N. Marchenkov, E. H. Conrad, P. N. First, and W. A. de Heer, Science **312**, 1191 (2006).
[7] K. V. Emtsev, A. Bostwick, K. Horn, J. Jobst, G. L. Kellogg, L. Ley, J. L. McChesney, T. Ohta, S. Reshanov, A. Rohrl, J. E. Rotenberg, A. Schmid, A. K. D. Waldmann, H. B. Weber, and T. Seyller, Nat. Mater. **8**, 203 (2009).
[8] W. Norimatsu and M. Kusunoki, Chem. Phys. Lett. **468**, 52 (2009).
[9] S. Y. Zhou, G. H. Gweon, A. V. Fedorov, P. N. First, W. A. de Heer, D. H. Lee, F. Guinea, A. H. Castro Neto, and A. Lanzara, Nat. Mater. **6**, 770 (2007).
[10] W. Norimatsu and M. Kusunoki, Phys. Rev. B **81**, 161410(R) (2010).
[11] Luxmi, N. Srivastava, G. He, R. M. Feenstra, and P. J. Fisher, Phys. Rev. B **82**, 235406 (2010).
[12] J. Kedzierski, P. L. Hsu, P. Healey, P. W. Wyatt, C. L. Keast, M. Sprinkle, C. Berger, and W. A. de Heer, IEEE Trans. Electron Devices **55**, 2078 (2008).
[13] J. L. Tedesco, B. L. VanMil, R. L. Myers-Ward, J. M. McCrate, S. A. Kitt, P. M. Campbell, G. G. Jernigan, J. C. Culbertson, C. R. Eddy, Jr., and D. K. Gaskill, Appl. Phys. Lett. **95**, 122102 (2009).
[14] C. Riedl, C. Coletti, T. Iwasaki, A. A. Zakharov, and U. Starke, Phys. Rev. Lett. **103**, 246804 (2009).
[15] D. Waldmann, J. Jobst, F. Speck, T. Seyller, M. Krieger, and H. Weber, Nat. Mater. **10**, 357 (2011).
[16] J. A. Robinson, M. Hollander, M. Labella III, K. A. Trumbull, R. Cavalero, and D. W. Snyder, Nano Lett. **11**, 3875 (2011).
[17] L. Muehlhoff, W. J. Choyke, M. J. Bozack, and J. T. Yates, J. Appl. Phys. **60**, 2842 (1986).
[18] G. G. Jernigan, B. L. VanMil, J. L. Tedesco, J. G. Tischler, E. R. Glaser, A. Davidson, III, P. M. Campbell, and D. K. Gaskill, Nano Lett. **9**, 2605 (2009).
[19] J. Hass, F. Varchon, J. E. Millan-Otoya, M. Sprinkle, N. Sharma, W. A. de Heer, C. Berger, P. N. First, L. Magaud, and E. H. Conrad, Phys. Rev. Lett. **100**, 125504 (2008).
[20] W. A. de Heer, C. Berger, X. S. Wu, P. N. First, E. H. Conrad, X. Li, T. Li, M. Sprinkle, J. Hass, M. L. Sadowski, M. Potemski, and G. Martinez, Solid State Commun. **143**, 92 (2007).
[21] X. Wu, Y. Hu, M. Ruan, N. K. Madiomanana, J. Hankinson, M. Sprinkle, C. Berger, and W. A. de Heer, Appl. Phys. Lett. **95**, 223108 (2009).
[22] J. L. Tedesco, G. G. Jernigan, J. C. Culbertson, J. K. Hite, Y. Yang, K. M. Daniels, R. L. Myers-Ward, C. R. Eddy, Jr., J. A. Robinson, K. A. Trumbull, M. T. Wetherington, P. M. Campbell, and D. K. Gaskill, Appl. Phys. Lett. **96**, 222103 (2010).
[23] W. Norimatsu, J. Takada, and M. Kusunoki, Phys. Rev. B **84**, 035424 (2011).
[24] W. A. de Heer, C. Berger, M. Ruan, M. Sprinkle, X. Li, Y. Hu, B. Zhang, J. Hankinson, and E. H. Conrad, PNAS Early Edition 16899.
[25] H. Hibino, H. Kageshima and M. Nagase, J. Phys. D: Appl. Phys. **43**, 374005 (2010).
[26] F. J. Ferrer, E. Moreau, D. Vignaud, D. Deresmes, S. Godey, and X. Wallart, J. Appl. Phys. **109**, 054307 (2011).
[27] D. Graf, F. Molitor, K. Ensslin, C. Stampfer, A. Jungen, C. Hierold, and L. Wirtz, Nano Lett. **7**, 238 (2007).
[28] C. Cong, T. Yu, K. Sato, J. Shang, R. Saito, G. F. Dresselhaus, and M. S. Dresselhausz, ACS Nano **5**, 8760 (2011).
[29] A. Venugopal, L. Colombo, and E. M. Vogel, Appl. Phys. Lett. **96**, 013512 (2010).
[30] K. Nagashio, T. Nishimura, K. Kita, and A. Toriumi, *IEEE International Electron Device Meeting (IEDM)* (IEEE, Piscataway, NJ, 2009), p. 565.
[31] J. A. Robinson, M. LaBella, M. Zhu, M. Hollander, R. Kasatda, Z. Hughes, K. Trumbull, R. Cavalero, and D. Snyder, Appl. Phys. Lett. **98**, 053103 (2011).